

# The nature of the radio-quiet compact X-ray source in SNR RCW 103

E. V. Gotthelf<sup>1,2</sup>, R. Petre<sup>1</sup> & U. Hwang<sup>1,3</sup>

<sup>1</sup> NASA/Goddard Space Flight Center, Code 660.2, Greenbelt MD, 20771, USA

<sup>3</sup> University of Maryland, College Park, MD, USA

## ABSTRACT

We consider the nature of the elusive neutron star candidate 1E 161348–5055 using X-ray observations obtained with the *ASCA* Observatory. The compact X-ray source is centered on the shell-type Galactic supernova remnant RCW 103 and has been interpreted as a cooling neutron star associated with the remnant. The X-ray spectrum of the remnant shell can be characterized by a non-equilibrium ionization (NEI) thermal model for a shocked plasma of temperature  $kT \sim 0.3$  keV. The spectrum falls off rapidly above 3 keV to reveal a point source in the spectrally-resolved images, at the location of 1E 161348–5055. A black-body model fit to the source spectrum yields a temperature  $kT = 0.6$  keV, with an unabsorbed 0.5–10 keV luminosity of  $L_X \sim 10^{34}$  erg s<sup>-1</sup> (for an assumed distance of 3.3 kpc), both of which are at least a factor of 2 higher than predicted by cooling neutron star models. Alternatively, a power-law model for the source continuum gives a steep photon index of  $\alpha \sim 3.2$ , similar to that of other radio-quiet, hard X-ray point sources associated with supernova remnants. 1E 161348–5055 may be prototypical of a growing class of radio-quiet neutron stars revealed by *ASCA*; we suggest that these objects account for previously hidden neutron stars associated with supernova remnants.

*Subject headings:* stars: individual (RCW 103, 1E 161348–5055) — stars: neutron — supernova remnants — X-rays: stars

## 1. Introduction

Neutron stars (NS) are thought to be born as the stellar remnants of supernova explosions involving massive star progenitors. It has long been assumed that NSs begin life as fast  $\sim 10$  ms radio pulsars emitting non-thermal radiation, with the Crab and Vela pulsars as the canonical examples. Thus it is remarkable that few ( $\sim 10$ ) of the  $\sim 200$  known Galactic SNR have pulsars associated with them (see Kaspi 1997), even though a large fraction of supernova explosions

---

<sup>2</sup>Universities Space Research Association

should have produced NSs. Perhaps we are seeing only those young SNR associated pulsars beamed in our direction or those with sufficiently large radio luminosities to have been detected (Lorimer 1993); or that pulsars are born with large “kick” velocities, launching them far from their remnants (Lyne & Lorimer 1994). But evidence of radio-loud “plerions” associated with young pulsars suggest they should be easily detectable near identified SNRs (Weiler & Sramek 1988). Here we present a radio-quiet NS candidate of moderate X-ray luminosity associated with the shell-type SNR RCW 103. Objects of this type may or may not share a common origin, but their lack of radio emission suggests that a reconsideration of pulsar evolution is needed; they might partially account for the missing young NSs associated with SNRs.

The X-ray source 1E161348–5055 was first detected with the high resolution imager (HRI) on-board the *Einstein* Observatory as a faint, unresolved source located near the center of RCW 103 (Tuohy & Garmire 1980). Although the location of 1E161348–5055 suggests an association with RCW 103, systematic optical and radio searches over the years were unable to find a counterpart (Tuohy & Garmire 1980, Tuohy *et al.* 1983, Dickel *et al.* 1996). A recent radio pulsar search using the Parkes radio telescope also produced a null result (Kaspi *et al.* 1996). With the lack of observational evidence for an accreting binary, Tuohy *et al.* (1983) initially proposed 1E161348–5055 as an isolated NS emitting thermal radiation, the first to be discovered. Subsequent observations using the imaging proportional counter (IPC) on-board *Einstein* failed to confirm its existence, ostensibly due to the IPC’s poor spatial resolution (Tuohy & Garmire 1980); and non-detections by the instruments on-board the *ROSAT* Observatory over the intervening years are attributed to degraded sensitivity of the off-axis target position (Becker *et al.* 1993). Until the present study, no systematic broad-band X-ray spectral analysis had been possible.

RCW 103 (G332.4-0.4) is an X-ray bright, nearly circular ( $\sim 9'$  diameter), shell-type Galactic SNR. Its distance is uncertain. Caswell *et al.* (1975) derived a value of 3.3 kpc from 21 cm Hydrogen line absorption measurements; an optical extinction study by Leibowitz & Danziger (1983) in the vicinity of RCW 103 yields a value of 6.6 kpc. Herein we adopt the former, more generally accepted, value, for consistency with previous studies. RCW 103 is similar to other young remnants in having a bright radio shell traced by the optical filaments (van den Bergh 1978; Dickel *et al.* 1996). Its small inferred diameter of ( $\sim 10$  pc) and the high velocity dispersion of its optical filaments ( $\sim 900$  km s $^{-1}$ ; Tuohy, *et al.*, 1979) are also consistent with a young ( $\sim 1000$  yrs) remnant (Nugent *et al.* 1984).

In this Letter we present confirmation of the existence of 1E161348–5055, characterize its spectrum, and reconcile the earlier non-detections with the *ASCA* data. Our detection is confirmed by a new *on-axis* *ROSAT* HRI observation recently made available in the public archive. In addition, we use spectral evidence from the nebula to portray a consistent picture of 1E161348–5055 as a young, Type II SNR with an embedded NS. We present 1E161348–5055 as proto-typical of a growing class of remnants with central radio-quiet NSs, which have hard spectra, but lack evidence for plerionic emission from a synchrotron nebula. Members of this class may also include CTB 109 (Corbet *et al.*, 1995), Puppis-A (Petre *et al.*, 1996), G296.5+10.0 (Mereghetti

*et al.* 1996) and Kes 73 (Gotthelf & Vasisht 1997).

## 2. Observations

A day-long observation of RCW 103 was performed using the *ASCA* Observatory (Tanaka *et al.* 1994) on Aug 17, 1993, during the Performance Verification (PV) phase of the mission. We used archival data from both pairs of on-board instruments, the solid-state spectrometers (SIS) and the gas scintillation spectrometers (GIS). The SIS detectors offer  $\sim 2\%$  spectral resolution at 6 keV (resolution  $\sim E^{-1/2}$  over its 0.4 – 12 keV bandpass). The spatial resolution is limited by the mirror point spread function (PSF), whose sharp core gives a FWHM of  $\sim 1'$  but large wings produce a half power diameter of  $\sim 3'$  (Jalota *et al.* 1993). These wings are problematic when extracting and modeling the spectrum of a point source embedded in diffuse emission. All SIS data were acquired in 4 CCD BRIGHT mode and screened using the standard REV1 processing.

We also extracted GIS data to search for pulsations and to help constrain the high energy spectrum. The GIS profits from more screened observing time and greater sensitivity above 2 keV than the SIS, but with poorer spectral ( $\sim 8\%$  at 6 keV) and spatial (FWHM  $\sim 3'$ ) resolution. The GIS data were collected in the highest time resolution mode (0.5 ms or 64  $\mu$ s, depending on data acquisition mode), with reduced spatial ( $1' \times 1'$  pixels) and spectral binning ( $\sim 12$  eV per PHA channel). A total of 47 ks of screened SIS data and 71 ks of screened GIS data were acquired from the observation.

Each SIS consists of four X-ray CCDs tiled in a square with a gap between each pair of chips. The  $22' \times 22'$  fields of view of the two instruments are slightly offset ( $\sim 1'$ ) in the direction of the larger of the two gaps. During this early PV observation, 1E161348–5055 was placed at an unfortunate location on the SIS, straddling the inter-CCD gaps. To compensate for aspect jitter near the gaps, we applied exposure corrections in constructing images. Figure 1 presents the unambiguous *ASCA* detection of 1E161348–5055, the first since its discovery. The hard-band ( $> 3.0$  keV) image (Fig. 1a) shows a distinct feature centered on the remnant, whose spatial distribution is consistent with that from a point source. In stark contrast, the soft-band (0.5 – 1.5 keV) image shown in Fig. 1b is dominated by diffuse emission from RCW 103, and reproduces low-resolution X-ray images of RCW 103 acquired with previous missions. Both images are centered on the bright peak in the hard-band map. 1E161348–5055 is also evident in the hard-band GIS image, albeit at the poorer spatial GIS resolution.

To locate 1E161348–5055 with improved accuracy we use the arcsec astrometry of the radio maps (Dickel *et al.* 1996) to register the SIS image of the remnant, which is found to correlate well with the radio morphology. The derived J2000 coordinates are R.A.  $16^h 17^m 35^s.5$ , Dec.  $-51^\circ 02' 21''$  degrees,  $7''$  away from the *Einstein* location, and within the expected offset of the combined *Einstein* error circle and *ASCA* measurement accuracy (see Gotthelf 1996). The centroid of the source is aligned with the radio depression and appears to be within an arc-minute of the inferred

radio center of the remnant.

In Figure 1 we also note the appearance of a faint X-ray source,  $\sim 7'$  due north of 1E161348–5055, which is confined to the hard-band image. The J2000 coordinates of the serendipitous source in the registered image are R.A.  $16^h17^m30^s.1$ , Dec.  $-50^\circ55'05$  degrees. No equivalent source at this location is apparent in any of the archival X-ray images of RCW 103. We checked the HEASARC catalogs and find no X-ray, radio, optical objects within  $3'$  of the detection. The absence of a source in the soft X-ray band-passes of the earlier missions may indicate that this source, which we designate AXS J161730 – 505505, is highly absorbed. Alternatively, the lack of a catalog ID suggests the discovery of a new transient or variable source.

Having demonstrated the presence of 1E161348–5055, we now use *ASCAs* full spectroscopic capability to infer some of its properties. This is not straightforward because the spectrum of the point source is superimposed on strong diffuse emission from the remnant, whose contribution to the source is increased due to the broad wings of *ASCAs* PSF. For the GIS, the situation is exacerbated by the reduced spatial resolution of the GIS detectors. Because of the increased diffuse emission in the larger extraction region required to sample the source, all attempts to fit the GIS spectrum produced unconstrained results, despite the GIS’s higher sensitivity at energies above 2 keV.

Our approach to fitting the SIS spectrum was to first characterize the remnant spectrum, and to use it as a “background” to fit the source spectrum. The combined source plus remnant spectrum was extracted from a small circular region  $2.4'$  in diameter, centered on the source to maximize the source signal. We used data from SIS-0 exclusively, as the point source abuts the inter-chip gap on SIS-1. For SIS-0, most of the source counts were collected on a single CCD chip. For a “background” field we extracted counts from this chip using a  $1.2'$  wide annular segment covering the bright SNR shell. An average sky background, made up of data from four surrounding archival blank survey fields, was subtracted from these spectra. We also generated custom response files for SIS-0 that take into account the restricted region we used. Systematic uncertainties are expected at the  $\sim 5\%$  level due to the azimuthal energy dependence of the PSF.

The shocked nebula plasma is evidently not in ionization equilibrium, as a single component Raymond-Smith ionization equilibrium plasma model does not adequately fit the spectrum. We used instead a non-equilibrium ionization (NEI) plasma model for Sedov hydrodynamics assuming  $T_e = T_{ion}$  (Hamilton, Sarazin & Chevalier 1983), in which the abundances of the elements were allowed to vary with C, N, O tied to each other and Fe tied to Ni. The spectrum is well fit with a single component model with temperature  $kT = 0.3$  keV and column density  $N_H = 7 \times 10^{21}$   $\text{cm}^{-2}$  (see Fig. 2a and Table I). The ionization parameter  $\eta \equiv n_o^2 E$  is  $10^{50}$  ( $\text{cm}^{-6}$  ergs), corresponding to an ionization age  $n_{et}$  of  $6 \times 10^3$   $\text{cm}^{-3}$  yr. Assuming a distance of 3.3 kpc, Sedov hydrodynamics gives an age of about 4000 yr for the remnant. This age represents an upper limit for a remnant in the adiabatic phase, and is consistent with the upper end of ages derived by Nugent *et al.* (1984).

We next fit for the source spectrum, using counts extracted from the region containing

emission from the source+remnant. The thermal “background” model alone, with only the normalization allowed to vary, gives an unacceptable fit (see Fig. 2b and Table I). As anticipated from the spectrally resolved images, there is a clear excess of counts above 2 keV. We then added in turn to the model one of three different continuum components — blackbody, power-law and thermal bremsstrahlung. Each of these greatly improves the fit, as detailed in Table I. In each case, we fixed the spectral parameters of the nebula except the Silicon abundance, for which there is evidence for slight variation with position. Only the normalization of the thermal component was allowed to vary. The column density was initially held fixed at the fit value for the nebula and then allowed to vary freely. All three continuum models yield comparable  $\chi^2$ . Except for the blackbody, the fits favor additional  $N_{\text{H}}$  for the point source (see Table I). This may be intrinsic absorption to the source or due to intervening, cold, clumped material near the SNR, serendipitously in the line of sight. The best fit black body model gives  $kT = 0.56$  keV, and the best fit power law model photon index is  $\Gamma = 3.2$  for fixed  $N_{\text{H}}$ , compared to  $kT = 0.57$  keV and  $\Gamma = 4.6$  for  $N_{\text{H}}$  freely fit.

The presence of a hard power-law component might signal an underlying pulsar. We searched the *ASCA* data for coherent modulation of the X-ray emission from the source at periods as short as 8 ms by performing a FFT on the GIS time series extracted from a circular region of radius  $4'$ . To minimize contamination from the supernova remnant, only counts with pulse heights corresponding to energies  $E > 2.6$  keV were used, resulting in a count rate of  $0.09 \text{ s}^{-1}$ , of which  $2/3$  are source counts and the other  $1/3$  arise from the SNR. We used a bin size of 4 ms and split the time series into four segments because of computational constraints. From the averaged power spectra of the four segments we find no significant power at 90% confidence at any of the frequencies searched. We searched the entire data set for periods greater than 2 s and find no modulations greater than 13% of the mean count rate, the limit of our sensitivity at the 90% confidence level. We also folded the light curve at the 69 ms period reported in IAUC 5588 and find no time modulation of the signal when compared to a null hypothesis ( $\chi^2_{\nu} \sim 1.0$ ).

We considered whether the source displays long-term variability by examining archival data. A total of 13 imaging observations of RCW 103 are available from the *Einstein*, EXOSAT, and *ROSAT* missions, spread-out fairly evenly over the 16 years since the detection of 1E161348–5055. Of these, three provide a detection: the discovery observation with the *Einstein* HRI, the *ASCA* observation presented here, and the recently released *on-axis ROSAT* HRI observation acquired in Aug 1995. We folded our model fits obtained with the *ASCA* spectra through the respective instrument spectral responses and compared their count rates using PIMMS (Mukai 1993). We first made comparisons using the best fit model parameters derived with fixed  $N_{\text{H}}$  (see Table I). For the *Einstein* and *ROSAT* HRI, whose observations span 16 years, we find that their background subtracted count rates agreed to within  $< 10\%$ . In contrast, all these fits predict a *ASCA* SIS count rate substantially higher than that observed, by a factor of three or more. One reason for the flux discrepancy may be the possibility that 1E161348–5055 is more highly absorbed than RCW 103. We again compared count rates this time using the model fit for which

$N_{\text{H}}$  were allowed to vary. The *ASCA* models then predict an HRI count rates  $\sim 2$  higher than measured. If we allow  $N_{\text{H}}$  to vary even higher, it is possible to obtain agreement, suggesting either strong intrinsic absorption or a factor of  $\sim 2$  variability of the flux.

As discussed in the next section, the relative count rates are very sensitive to the instrumental energy band-pass, along with the assumed  $N_{\text{H}}$ . Given the uncertainties in the *ASCA* spectrum and flux due to the nebular contamination below 2 keV, it is unclear that the source varies significantly. A set of internally consistent measurements (i.e., with the same instrument) will be needed to establish variability.

### 3. Discussion

The *ASCA* observation suggests two reasons why 1E161348–5055 has been so difficult to detect in previous observations: its hard spectrum is obscured in the soft X-ray band by the nebular flux, and intrinsic absorption may reduce its soft flux in the *ROSAT* band-pass. At energies above 2.5 keV the source spectrum is clearly dominant over the soft thermal flux of the nebula (see Fig 2b). Detecting an unresolved point-source embedded in a significant background is highly dependent on the beam-size and energy. The *ROSAT* band-pass is limited by the mirror response to  $< 2.0$  keV, whereas the *Einstein* response continues to  $\sim 4.5$  keV. Although the *ASCA* beam-size is much greater than that of the on-axis HRI PSF (beam-size  $\sim 5''$ ), the increased high energy response up to  $\sim 10$  keV allows direct imaging of the hard component above  $\sim 2$  keV. For the *ROSAT* HRI observations made with the target off-axis, the increased beam-size ( $\sim 1'$  vs.  $5''$ ) and mirror vignetting ( $\sim 15\%$ ) reduced the detectability of the faint *Einstein* HRI source to below threshold (see Becker 1993). The large intrinsic instrumental blur of the *Einstein* IPC and the *ROSAT* PSPC also reduce the point-source sensitivity.

In the following we reconsider the main observational arguments concerning a cooling neutron star origin, an accreting binary, or a plerionic origin for 1E161348–5055. None of these are found to be completely satisfactory and so we examine alternative origins for the compact source in RCW 103. Based on the *Einstein* discovery observation, 1E161348–5055 was suggested to be an isolated cooling NS dominated by thermal emission. Indeed, several SNR contain intriguing cooling NS candidates, including Puppis A (Petre *et al.*, 1996) and G296.5+10.0 (Mereghetti *et al.*, 1996). Although the *ASCA* spectrum allows a blackbody solution, the temperature and luminosity are hard to reconcile with current theoretical models (see Ögelman 1995 for a review), which may well require reconsideration, perhaps by allowing for an accreted envelope (see Chabrier *et al.* 1997 and references therein).

The morphology of RCW 103 is inconsistent with a plerion dominated by synchrotron emission, such as is observed from Crab-like composite remnants. The central sources in these young ( $< 1000$  yrs) SNR are copious radio emitters with highly polarized extended synchrotron nebulae driven by a radio pulsar (Dickel *et al.* 1994). Their non-thermal cores produce X-ray

spectra with hard power-law photon indices of  $\sim 2$ . Alternatively, some young shell-type SNRs are thought to contain a faint plerionic core, such as G 11.2–0.3 (Vasisht *et al.* 1996). Although the remnant of this young SNR is similar to that of RCW 103, the embedded radio source likely requires a different origin; perhaps the radio source is at a different evolutionary stage.

The evidence against an accreting binary is equally compelling. The luminosity range for a typical accretion-driven low-mass X-ray binary (LMXB) is  $\sim 10^{36-38}$  ergs s $^{-1}$ , implying a distance for 1E161348–5055 far behind those estimated for RCW 103. As noted by Tuohy *et al.* (1983), the soft thermal nebular spectrum is incompatible with the implied interstellar column density at that distance. For a binary origin for 1E161348–5055, we would expect to find an optical companion, perhaps with ultraviolet excess from an accretion disk, displaying Doppler shifted optical absorption lines.

The properties of RCW 103 along with its compact source are quite similar to other radio-quiet compact X-ray sources found near the center of SNRs probed by *ASCA*. These sources are identified by their X-ray emission in the hard band-pass, above the shocked thermal remnant emission. In particular, RCW 103 is most similar to Kes 73. Both are young, distant Type II Galactic SNRs with comparable thermal spectra and apparent morphologies. Unlike G 11.2–0.3, both RCW 103 and Kes 73 contain central radio-quiet X-ray sources with similar spectral properties (see Gotthelf & Vasisht 1997). Furthermore, neither shows evidence for a radio or optical counterpart, or for plerionic X-ray emission. Kes 73 contains a 12 s X-ray pulsar which is likely being spun down quickly by virtue of an anomalously large magnetic field (see Vasisht & Gotthelf 1997 and ref. therein). The most striking difference between the two systems is the luminosity of the compact source. The younger ( $\sim 1000$  yrs) and hotter (kT  $\sim 0.7$  keV) Kes 73 emits a larger fraction of its flux from the compact source ( $\sim 4 \times 10^{35}$  ergs s $^{-1}$ ) relative to the shell, as might be expected for a younger system radiating energy at a higher rate, perhaps due to the large postulated magnetic field.

The luminosity and age of 1E161348–5055 are also consistent with an isolated pulsar radiating gravitational energy. The maximum luminosity for a  $\sim 2000$  yr old,  $\sim 10$  s pulsar powered by spin-down energy is in the range of  $\sim 10^{33-34}$  erg s $^{-1}$ , for a  $1.4M_{\odot}$  neutron star. Perhaps the pulsar has spun down, radiating residual braking energy and is sub-luminous for a plerion, but hotter and brighter than a quiescent cooling NS. If RCW 103 is typical of SNR with radio quiet, non-plerionic central compact sources, this may well explain the mysterious absence of observed natal NSs associated with Type II SNR. In this scenario pulsars with strong magnetic fields are spun-down rapidly, losing their adolescent radio plerionic nebulae and slowly dim. We hope that further multi-wavelength studies will help elucidate the significance of this intriguing object.

**Acknowledgments** — This work uses data made available from the HEASARC public archive at GSFC. We are indebted to J. Dickel for kindly providing us with his radio maps of RCW 103, C. M. Becker for use of his timing analysis software, and V. M. Kaspi for discussion.

## REFERENCES

- Becker, W., Trümper, J., Hasinger, G., & Aschenbach, B. 1993 in “Isolated Pulsars”, ed Van Riper, Epstein, & Ho, Cambridge Univ. Press (Cambridge), 116.
- Caswell, J. L., Murray, J. D., Roger, R. S., Cole, D. J., & Cooke, D. J. 1975, AA, 45, 239.
- Chabrier, G., Potekhin, A. Y., & Yakovlev, D. G., 1997 ApJ, 477, L99.
- Corbet, R. H. D., Smale, A. P., Ozaki, M., Koyama, K., & Iwasawa, K. 1995, ApJ, 443, 786.
- Dickel, J. R., Milne, D. K., Kennicutt, R. C., Chu, Y-H., Schommer, R. A. 1994, AJ, 107, 1067.
- Dickel, J. R., Green, G., Ye, T., & Milne, D. K. 1996, AJ, 111, 340.
- Gotthelf, E. V. 1996, ASCAnews 4, 31.
- Gotthelf, E. V. & Vasisht, G. 1997, ApJL in press, astro-ph/9706057.
- Hamilton, A. J. S., Sarazin, C. L., & Szymkowiak, A. E. 1983, ApJS, 51, 115.
- Jalota, L., Gotthelf, E. V. & Zoonermatkermani, S. 1993, Proc. SPIE, 1945, 453.
- Kaspi, V. M. 1996, ‘in “IAU Colloquium 160 Pulsars: ‘Problems and Progress’ conference proceedings, ed S. Johnston, M. Bailes & M. Walker, ASP Conference Series, 105, 375.
- Kaspi, V. M., Manchester, R. N., Johnston, S., Lyne, A. G., & D’Amico, N. 1996 AJ, 111, 2028.
- Leibowitz, E. M. & Danziger, I. J. 1983, MNRAS, 204, 373.
- Lorimer, D. R., Bailes, M., Dewey, R. J., Harrison, P. A. 1993, MNRAS 263, 403.
- Lyne, A. G. & Lorimer, D. R. 1994, Nature, 369, 127.
- Mukai, K. 1993, Legacy 3, 21.
- Mereghetti, S. Bignami, G. F., & Caraveo, P. A. 1996, 464, 842.
- Nugent, J. J., Becker, R., H., Garmire, G. P., Pravdo, S. H., Touhy, I. R., Winkler, Jr., P. F. 1984, ApJ., 284, 612.
- Ögelman, H. 1995, *Proceedings of the NATO ASI on the Lives of NSs*, eds. Alpar, A., Kiziloglu, Ü., & van Paradijs, J., Kluwer, Dordrecht.
- Petre, R., Becker, C. M., Winkler, P. F. 1996, 465, L43.
- Tanaka, Y., Inoue, H., & Holt, S. S. 1994 PASJ, 46, L37.
- Tuohy, I. R., Mason, K. O., Clark, D. H., Córdoba, P. A. Charles, Walter, F. M., & Garmire, G. P. 1979, ApJ, 230, L27.
- Tuohy, I. R. & Garmire, G. P. 1980, ApJ, 239, L107.
- Tuohy, I. R., Garmire, G. P., Manchester, R. N., & Dopita, M. A. 1983, ApJ, 268, 778.
- Vasisht, G. & Gotthelf, E. V. 1997, ApJL in press, astro-ph/9706058.
- van den Bergh, S. 1978, ApJS, 38, 119.



Weiler, K. W. & Sramek, R. A. 1988, *ARA&A*, 26, 29.

Table 1. Fits to the *ASCA* SIS Spectra

Model	$\chi^2(\text{DoF})$	kT or $\Gamma$	$N_H$ ( $10^{22} \text{ cm}^2$ )	Flux ( $\times 10^{-11} \text{ cgs}$ )
Nebula NEI	77 (77)	0.3	0.68	-
Source NEI	517 (93)	-	-	-
— Fits to source with $N_H$ fixed —				
NEI + BB	105 (99)	$0.56_{0.53}^{0.59}$	0.68	0.62
NEI + PL	130 (99)	$3.2_{3.0}^{3.4}$	0.68	1.8
NEI + BREM	110 (99)	$1.6_{1.4}^{1.8}$	0.68	1.0
— Fits to source with $N_H$ free —				
NEI + BB	104 (98)	$0.57_{0.52}^{0.62}$	$0.5_{0.0}^{1.1}$	0.56
NEI + PL	106 (98)	$4.6_{4.0}^{5.3}$	$3.1_{2.1}^{4.3}$	1.7
NEI + BREM	103 (98)	$1.2_{1.0}^{1.5}$	$1.6_{1.0}^{2.4}$	1.6

For the nebula fit the abundances of the elements were allowed to be fit with C, N, O tied to each other and Fe tied to Ni.  $\text{Log } \eta$  ( $\text{cm}^{-6} \text{ ergs}$ ) = 50. All subsequent fits used the nebula NEI model fixed with only the normalization allowed to vary.  $\Gamma$  is the photon spectral index; kT in units of keV. Flux refers to the unabsorbed flux of the second component in the 0.5 – 10 keV band.

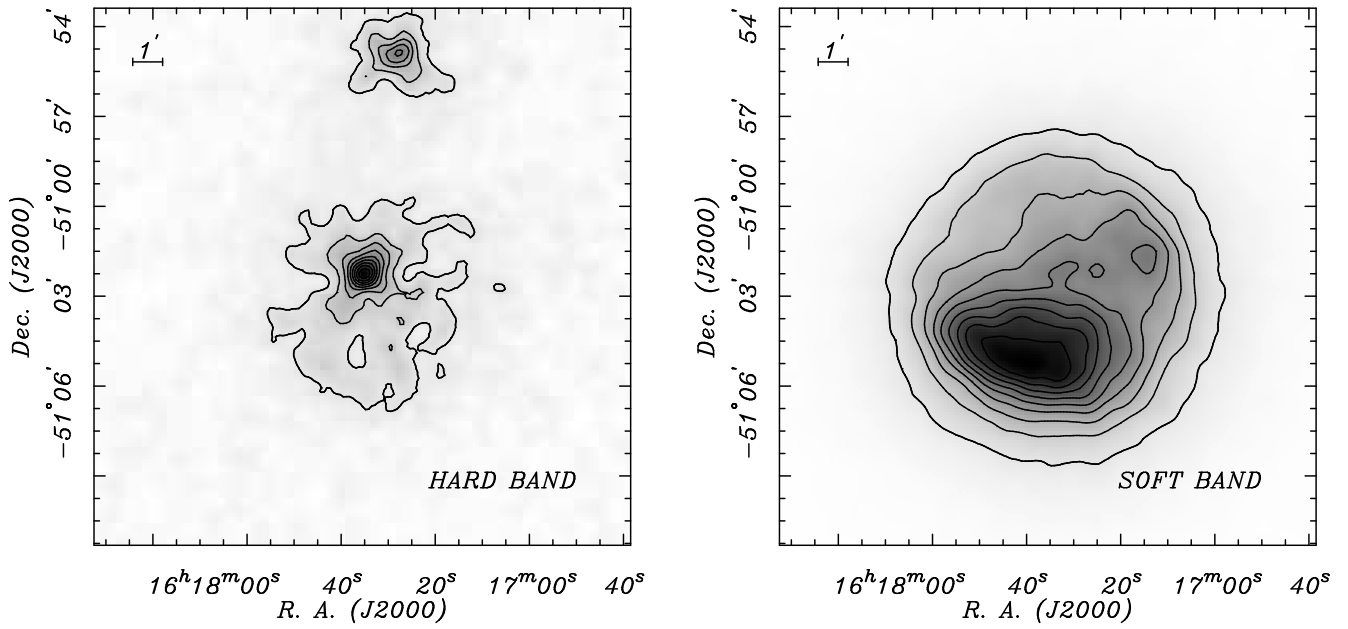


Fig. 1.— Exposure corrected and smoothed *ASCA* SIS images of RCW 103. a) The hard-band ( $> 3.0$  keV) SIS image of RCW 103 shows the unambiguous *ASCA* detection of 1E 161348–5055; the spatial distribution is consistent with that of a point source. b) The soft-band (0.5 – 1.5 keV) image is consistent with previous imaging observations of RCW 103. In this band-pass the nebula emission dominates the flux from 1E 161348–5055. The images are displayed with a linear greyscale and contours in 10 equal intervals.

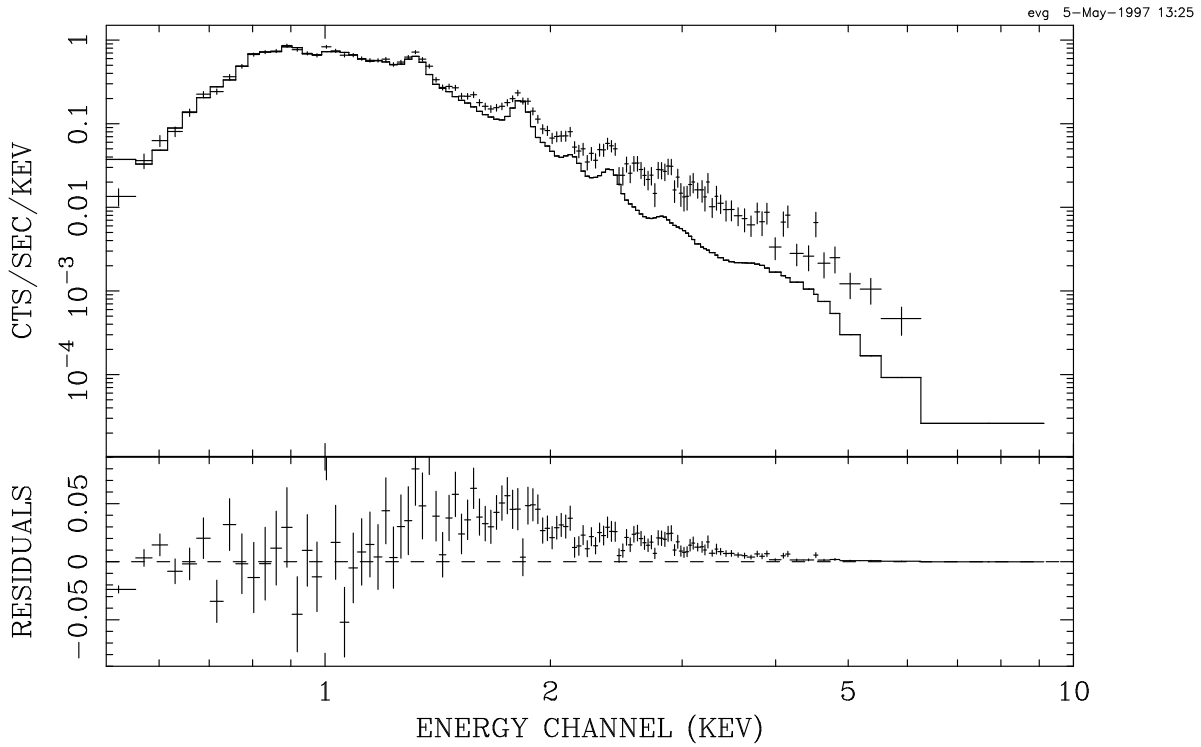
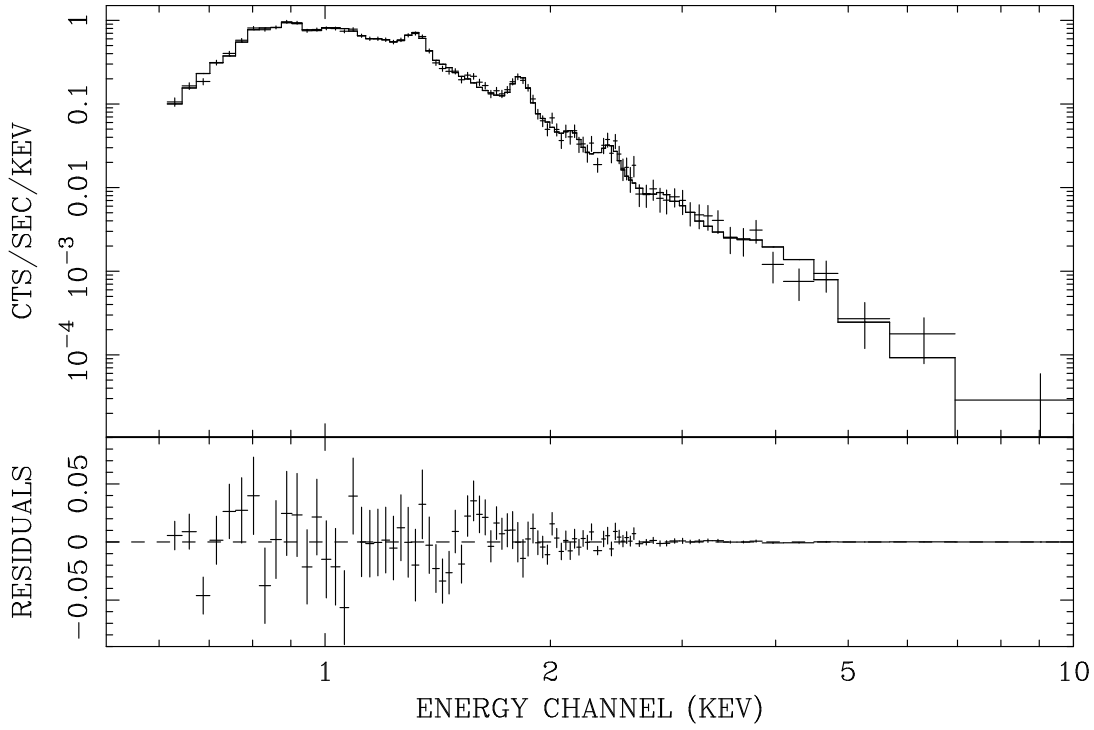


Fig. 2.— The *ASCA* SIS spectrum of RCW 103 showing (a) the fitted nebula spectrum and (b) the same model overlaid on the source spectrum to highlighting the 1E161348–5055 component.